Article

Relay-Like Exchange Mechanism through a Spin Radical between TbPc Molecules and Graphene/Ni(111) Substrates

Simone Marocchi, Andrea Candini, David Klar, Willem Van den Heuvel, Haibei Huang, Filippo Troiani, Valdis Corradini, Roberto Biagi, Valentina De Renzi, Svetlana Klyatskaya, Kurt Kummer, Nicholas B. Brookes, Mario Ruben, Heiko Wende, Umberto del Pennino, Alessandro Soncini, Marco Affronte, and Valerio Bellini

ACS Nano, **Just Accepted Manuscript** • DOI: 10.1021/acsnano.6b04107 • Publication Date (Web): 11 Oct 2016

Relay-Like Exchange Mechanism through a Spin Radical between $TbPc_2$ Molecules and Graphene/Ni(111) Substrates

Simone Marocchi,[*,†,‡] Andrea Candini,[*,†] David Klar,[¶] Willem Van den Heuvel,[§] Haibei Huang,[§] Filippo Troiani,[†] Valdis Corradini,[†] Roberto Biagi,[‖,†] Valentina De Renzi,[‖,†] Svetlana Klyatskaya,[⊥] Kurt Kummer,[#] Nicholas B. Brookes,[#] Mario Ruben,[⊥,@] Heiko Wende,[¶] Umberto del Pennino,[‖,†] Alessandro Soncini,[*,§] Marco Affronte,[‖,†] and Valerio Bellini[*,†]

†*S3 - Istituto Nanoscienze - CNR, Via Campi 213/A, 41125 Modena, Italy*
‡*Universidade de Sao Paulo - IFSC Av. Trabalhador são-carlense, 400 , São Carlos, Brazil*
¶*Faculty of Physics and Center for Nanointegration Duisburg-Essen (CENIDE), University of Duisburg-Essen, Lotharstrasse 1, D-47048 Duisburg, Germany*
§*School of Chemistry, University of Melbourne, VIC 3010, Australia*
‖*Dipartimento di Scienze Fisiche, Matematiche e Informatiche, Universitá di Modena e Reggio Emilia, Via Campi 213/A, 41125 Modena, Italy*
⊥*Institute of Nanotechnology, Karlsruhe Institute of Technology (KIT), D-76344 Eggenstein-Leopoldshafen, Germany*
#*European Synchrotron Radiation Facility (ESRF), Avenue des Martyrs 71, 38043 Grenoble, France*
@*Institut de Physique et Chimie des Materiaux de Strasbourg, UMR 7504 UdS-CNRS, 67034 Strasbourg Cedex 2, France*

E-mail: simonemarocchi@ifsc.usp.br; andrea.candini@nano.cnr.it; asoncini@unimelb.edu.au; valerio.bellini@nano.cnr.it

Abstract

We investigate the electronic and magnetic properties of $TbPc_2$ single ion magnets adsorbed on a graphene/Ni(111) substrate, by density-functional theory (DFT), *ab-initio* complete active space self-consistent field calculations, and x-ray magnetic circular dichroism (XMCD) experiments. Despite the presence of the graphene decoupling layer a sizable antiferromagnetic coupling between Tb and Ni is observed in the XMCD experiments. The molecule-surface interaction is rationalized by the DFT analysis and is found to follow a relay-like communication pathway, where the radical spin on the organic Pc ligands mediates the interaction between Tb ion and Ni substrate spins. A model Hamiltonian which explicitly takes into account the presence of the spin radical is then developed, and the different magnetic interactions at play being assessed by first-principle calculations and by comparing the calculated magnetization curves with XMCD data. The relay-like mechanism is at the heart of the process through which the spin information contained in the Tb ion is sensed and exploited in carbon-based molecular spintronics devices.

Keywords: molecular magnetism; graphene; spintronics; density functional theory; metal-organic interface

Single ion magnets belonging to the family of bis(phthalocyaninato) lanthanide (Ln) double-decker complexes ($LnPc_2$, with Pc = phthalocyanine) emerged recently as promising molecular spin units, where both the electronic and nuclear spin information can be addressed and, under certain experimental conditions, manipulated by external electric and magnetic stimuli, thus constituting a molecular brick for spintronic devices.[1–3]

Among them, $TbPc_2$ has been so far the most studied molecule, starting from the pioneering work of Ishikawa.[4,5] In its neutral form, the spin-orbital moment hosted by the f-electrons is flanked by a radical spin S=1/2, which delocalizes onto the two Pc ligands. It has been shown that the f magnetic moment in this class of molecules can couple to ferromagnetic and antiferromagnetic surfaces.[6] These are remarkable findings, if one considers that the Tb ion is shielded by the organic Pc ligands, in contrast to flat 3d-metal phthalocyanines or porphyrins,[7–9] where the ion is drawn in direct contact with the surface.

There is a general consensus in considering the magnetic coupling between the f electrons and a substrate/electrode as occurring not simply through space (dipolar). The orbitals of the Pc rings act as a bridge between the f spins and substrate magnetization, allowing for magnetic exchange. It has been suggested that in order for the localized f-electrons to communicate/hybridize with the outer world, here represented by the N and C sp electrons of the Pc rings, an important role is played by the d-electrons of the Ln ions.[10,11] Early NMR experiments[12] provided clear evidences of the presence of an S=1/2 radical in polycrystalline samples of YPc_2, and the interaction between the radical and the f magnetic moment has been clearly demonstrated by comparing the results of the neutral form of $TbPc_2$ with those of the anionic form $[TbPc_2]^-[TBA]^+$ in spintronic devices.[3] An unresolved issue is if the radical spin in the Pc rings endures upon deposition on a substrate. Previous analyses have relied on scanning-tunneling spectroscopy (STS) and microscopy (STM) experiments, where the interaction between the $TbPc_2$ molecules and non-magnetic, Cu,[13] Au,[14] carbon nanotubes[3] and magnetic, *i.e.* Co,[15] substrates has been studied. The evidence is that only on low interacting Au or carbon nanotube surfaces spin polarized states at the Pc rings are still present. Yet, the dilemma whether the spin in the Pc rings exists in the form of a self-standing radical or is due to contact interaction with magnetized substrates still remains unsettled. To address this issue, one should ideally have a substrate, which is scarcely reactive, so that the magnetic properties of the $TbPc_2$ molecule are preserved, and yet hosts a net magnetization, leading to a measurable exchange coupling with the molecular spins.

Here we present a combined theoretical and experimental investigation of the interaction between $TbPc_2$ molecules and graphene/Ni(111) substrates. By low-temperature XMCD experiments, we give evidence for an antiferromagnetic interaction between the molecule and the substrate, *i.e.* between the Tb and Ni magnetic moments. Density-functional theory calculations are carried out for the whole molecule-substrate system, in order to shed light on the mechanism behind this interaction, addressing the charge transfer at the interface. We observe that, in virtue of the graphene decoupling layer, the electron transfer occurring at the molecule-substrate is reduced, and, although sizable, is such that the radical spin is preserved. Placing the $TbPc_2$ molecule in direct contact with the Ni substrate leads instead to the destruction of radical, while spin polarized states are induced at the lower Pc ring by contact interaction. We can thus propose a model Hamiltonian which takes into account explicitly the spin radical, describes the relay-like spin communication between the 4f electrons and the magnetized Ni substrate, and reproduces the magnetization curves extracted by XMCD. Furthermore, the model considers the multi-domain magnetic character of the Ni single crystal used in our experiments. Finally, by multi-configurational Complete Active Space Self Consistent Field (CASSCF/RASSI–SO) and DFT calculations we estimate the various magnetic interactions at play, and discuss them in light of the existent experimental evidences.

Results

The existence of an exchange coupling between the Tb spins and the Ni magnetization has been demonstrated by experimentally measuring the magnetic properties of $TbPc_2$ molecules evaporated on a graphene/Ni(111) substrate, which we present hereafter. After preparing the graphene/Ni(111) surface according to the same procedure we have already reported,[9] we thermally evaporate 0.2-0.3 monolayer of $TbPc_2$ molecules. Experiments were carried out at the ID8 (now ID32) beamline of the European Synchrotron Radiation Facility (ESRF) in Grenoble. A schematic view of the experimental conditions can be seen in the inset of Figure 1: the external magnetic field **B** was applied parallel to the incident photon beam with an angle Θ with the sample surface ($\Theta = 0°$ defines the normal incidence direction). X-ray Natural Linear Dichroism (XNLD) measurements on the Tb $M_{4,5}$ and N K edges (shown on the Supporting Information) indicate that the $TbPc_2$ molecules are isolated and flat on the substrate, with the Pc plane parallel to the surface, in agreement with previous works on $TbPc_2$.[8,16–21] Figure 1 shows XAS absorption and XMCD spectra at the $M_{4,5}$ absorption edges of Tb taken at T = 8 K and B = 5 T. In agreement with previous works,[8,16–21] spectra taken at an angle of $\Theta = 0°$ (a) and $\Theta = 70°$ (b), while displaying the same lineshapes, show a remarkable dependence of the XMCD intensity on the field direction, which is a direct consequence of the strong uniaxial anisotropy of the $TbPc_2$ molecules.

The magnetization cycles of the $TbPc_2$ molecules adsorbed on the graphene/Ni(111) surface, extracted measuring the XMCD signal as a function of the external magnetic field, are shown in Figure 2 for a magnetic field applied perpendicular ($\Theta = 0°$) and at grazing ($\Theta = 70°$) incidence. Interestingly, the curve taken at $\Theta = 70°$ displays a kink (see inset in Fig. 2) which is the signature of the antiferromagnetic coupling with the underlying Ni substrate, consistent with what has been recently reported by Lodi Rizzini *et al.*[16] and our group,[9] when the molecule is directly adsorbed on Ni(111) substrates. Here, however, the intensity of the coupling is much reduced due to the presence of the graphene interlayer.

In order to unravel the mechanisms behind the molecule-substrate magnetic interaction, we performed DFT calculations, using the Quantum Espresso code[22] (computational details are given in the Methods section). In Fig. 3 we sketch the atomic structure of the molecule-substrate interaction region, and highlight the three magnetic units at play, *i.e.* Tb magnetic moment (yellow arrow), organic spin radical (green arrows), and Ni magnetization (blue arrows). The eight f electrons of the Tb ion, according to the Hund's rules, arrange into orbitals as to maximize both the total spin and angular momentum (S=3 and L=3), which are coupled and aligned parallel to each other due to spin-orbit interaction. The Tb ion acquires a 3+ valence, giving three electrons to the π-conjugate systems of the Pcs, which in turn tend to acquire a $-2\,e^-$ charge each. The unbalanced electron leads to a spin polarized radical equally distributed, in the gas-phase molecule, on the two Pc rings. The spin density of the gas-phase $TbPc_2$ molecule is plotted in Figure 4(a), in the case that the Tb and the radical spins are antiferromagnetically coupled to each other. It can be noticed that the spin density on the Pcs is mainly localized on the inner 16 C atoms (on average 0.05 μ_B/C atom) nearest to the Tb ion, the remanent polarization being on the outer C atoms (0.005 μ_B/C atom), while a small negative polarization is observed on the N atoms (about -0.01 μ_B/N atom). Finally, the magnetization of the graphene/Ni(111) substrate has to be considered.

Various theoretical and experimental research groups have investigated the structure and magnetic properties of graphene deposited on a surface of Ni(111) and identify, as the more frequent, two possible stacking configurations[23–25] labeled as top-fcc (the graphene C atoms alternately place themselves over the atoms of the first and third layer of Ni) and top-bridge (the graphene C atoms lie in a bridge positions between the atoms of the first layer of Ni). In both of them, the bonding between graphene and the Ni(111) surface is primarily due to extended

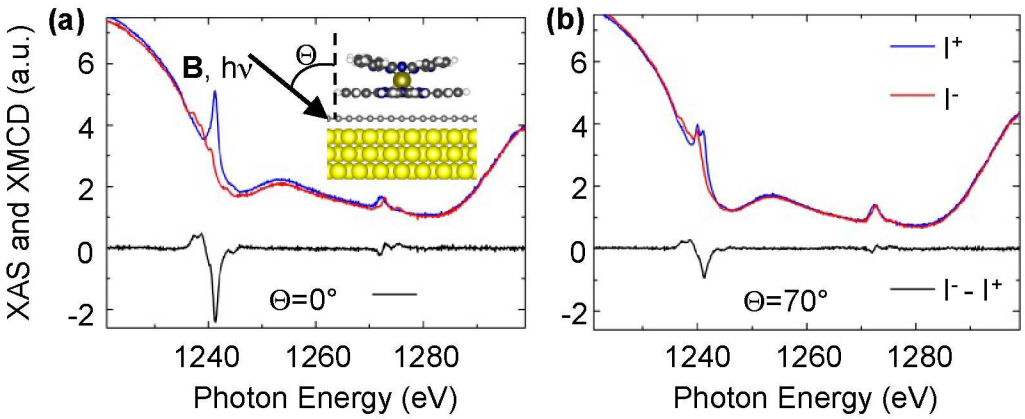

Figure 1: XAS (red and blue, for the two different light polarizations) and XMCD spectra (black) for Tb $M_{4,5}$ edge in $TbPc_2$/graphene/Ni(111) at $\Theta = 0°$ (a) and $\Theta = 70°$ (b) incidence angles, measured with an applied external field of 5 T.

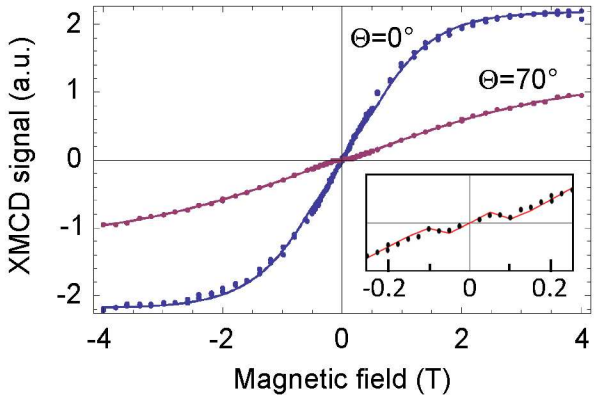

Figure 2: XMCD magnetization of $TbPc_2$ on the graphene/Ni(111) substrate, for $\Theta = 0°$ (blue dots) and $\Theta = 70°$ (red dots). The lines are the simulated Tb magnetizations using Hamiltonian (1) (see later in the text)). In the inset a zoom-up of the low-field region for the $\Theta = 70°$ case is displayed.

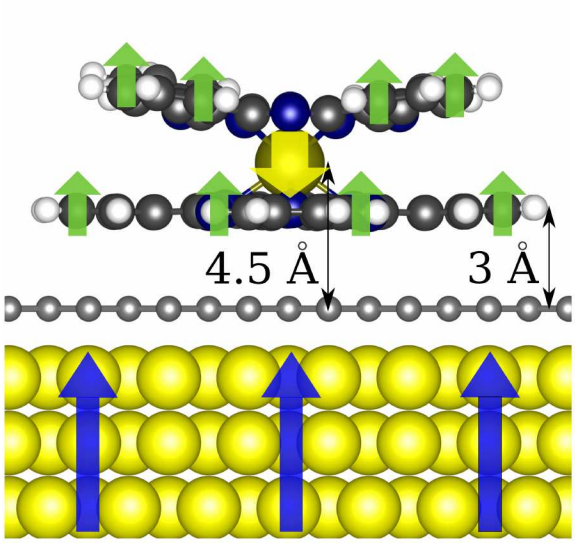

Figure 3: Adsorption geometry of the $TbPc_2$ on graphene/Ni(111). The C, N, H, are colored dark gray, dark blue and white, respectively, while the Tb ion is in green. The arrows represent the three different spins: the Tb, the radical on the Pcs and the Ni slab, colored yellow, green and blue, respectively. The orientation of the spins is the one attained in the ground state, as calculated by DFT.

van der Waals (vdW) interactions, with a binding distance of $\approx$ 2.1 Å. In the top-fcc stacking, a small spin polarization (around 0.02-0.03 Bohr magneton in modulus) is induced by the Ni spins on the graphene layer, with opposite sign on the two inequivalent C atoms, while in the top-bridge stacking the spin polarization is one order of magnitude smaller and of the same sign on the two C atoms.[9,26] In the following we discuss in detail the top-fcc stacking (the most abundant, *i.e.* $\simeq$ 65%), while results for the top-bridge stacking are shown in the Supporting Information.

We consider $TbPc_2$ molecule aligning with the Pc parallel to the surface, as indicated by XLND experiments, and the case where the Tb spin is coupled antiferromagnetically to the Pc radical, which in turn is parallel to the Ni magnetization direction, as depicted in Fig. 3. The structural optimization of the system teaches us that, upon adsorption, the $TbPc_2$ undergoes a series of structural changes (compare panels (a) and (c) in Fig. 4). In particular, it can be noticed a flattening of the curvature of the Pc in contact with the graphene, while the upper Pc bends outward from the surface. The flattening of the lower Pc is due to van der Waals interactions between the instantaneous induced multipoles in the π-conjugate systems of the Pc and the graphene/Ni substrate, leading to an average Pc-graphene distance of around 3 Å, while the bending of the upper Pc is due to charge repulsion between the two Pc's. The Tb ion stands at 4.5 Å from the graphene layer, leading to an overall Tb-Ni distance of more than 6.6 Å. Upon deposition, charge transfer of 0.75 e^- from the molecule to the surface takes place, and a partial quenching of the Pc spin radical is observed, its moment dropping to around 0.2 μ_B. No visible alteration is observed for the spin moment of Tb. In panels (b) and (c) of Fig. 4 top and side views of the spin density isosurface are presented. Together with the known alternating spin polarization at the graphene layer, a sizable quenching of the spin polarization can be observed in the upper Pc plane, together with a reduction of the polarization in the Pc plane close to the substrate.

More insight can be gained analyzing the

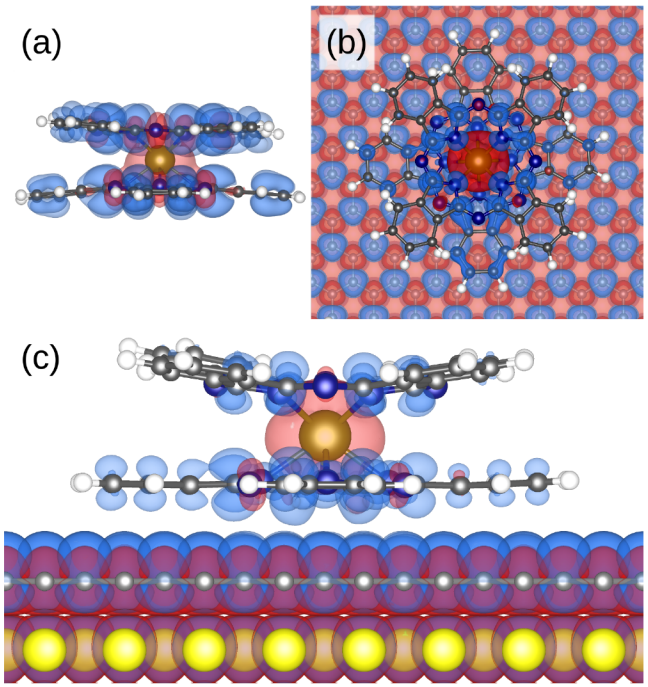

Figure 4: Spin density plot for $TbPc_2$ in the gas phase (a) and after the adsorption on graphene/Ni(111) for the top-fcc stacking, the top view (b) and side view (c), for the spin configuration depicted in Fig. 3. The spin up and down excesses are depicted in blue and red for isovalues of 0.0003 electrons/a.u.^{3}. Ni has an inner (blue) core of spin up excess electrons, which is surrounded by spin down electrons, the superposition of which giving a violet coloration in the figure.

projected local density of states (LDOS) of the $TbPc_2$, in the gas phase and absorbed on graphene/Ni, as shown in Figure 5, where we plot the states with f and d orbital character of the Tb ion, as well as the p-states of the N and C ions in the Pc closer to the Tb ion, together with the LDOS of the substrate, *i.e.* p_z-states at the graphene and d_{z^2}-states of the topmost Ni layer. Focusing on the space distribution of spin-polarized LDOS of the gas-phase $TbPc_2$ molecule we notice that the majority spin highest-occupied molecular orbital (HOMO) is localized mainly on the first circle of C and N atoms around the Tb (enlarged atoms in the sketch of Figure 5). The HOMO is shown as a light grey peak close to Fermi level (E_F) in Figure 5(b). Comparing the LDOS of the Pcs before (Fig. 5(b)) and after (Fig. 5(d)) the adsorption on graphene/Ni(111), we can see a rearrangement of the states closer to E_F due to the hybridization between the $2p$ states of Pcs and the $2p_z$ states of graphene, accompanied by a small shift to lower energies of the molecular C and N ($2p$) and Tb ($3d$) orbitals. On the one hand, being these spin polarized orbitals of the Pc the ones associated with the spin radical, it is clear that their hybridization with the substrate is detriment for the radical's survival. On the other hand, it is interesting to note that in case of semiconducting or insulating decoupling layers a complete loss of hybridization would eventually take place, with disruptive effects on the magnetic coupling. We can thus conclude that a small amount of hybridization is optimal for preserving the spin radical, and, at the same time, enabling its magnetic coupling with the substrate. The partial metallicity assumed by graphene through the interaction with the Ni substrate seems to supply the correct amount of hybridization. Not much could be said on the Tb f orbitals, since they are only poorly altered upon adsorption, due to their localized character. The survival of the spin radical upon adsorption, which we observe here, is a non obvious finding and is directly related to the presence of the graphene decoupling layer.

To confirm this, we performed calculations for a $TbPc_2$ molecule directly adsorbed on a Ni(111) slab. The interaction with the substrate leads, similarly to what has been found in the presence of the graphene layer, to a general flattening of the lower Pc ring, while the H atoms are pushed away from the surface due to steric repulsions. The distance between the Pc and the upper Ni atoms is around 1.97 Å, being the interaction much stronger, as compared to the 3 Å distance between the Pc and graphene. This reflects in a larger charge transfer from the molecule to the surface and the complete quenching of the radical spin. The interaction with the reactive Ni surface leads instead to a robust polarization of the lower Pc plane induced by contact interaction with the Ni substrate (see Fig. 6). The spin polarization changes sign across the lower Pc ring, and arises from contact interaction with the spin-polarized Ni surface. On the other hand, in the case of the graphene/Ni substrate discussed above, the spin radical could be stabilized in two metastable spin solutions, *e.g.* either parallel (which is the state of lowest energy, as it will be discussed later) or antiparallel with respect to the Ni magnetization. We also note that if the twist angle between the upper and lower Pc planes is around 41-42° in the molecular crystal,[27] and it is close to 45° in our gas-phase calculations, it is reduced to 41° when the molecule is deposited on the graphene/Ni surface, while is sensibly smaller when the molecule interacts directly with the Ni surface, *i.e.* $\simeq 36°$. Thus, the increase of the molecule-surface charge transfer is associated with a reduction of the twist angle between the Pc planes, which comes hand in hand with the quenching of the spin radical, as suggested by Komeda *et al.*[14]

The above analysis entails in a natural way the idea that the interaction mechanism which takes place between Tb and Ni could differ, depending on whether the spin radical in the Pc is suppressed or not. Experiments on rare-earth double deckers directly adsorbed on Ni(111) presented earlier[16] and recently confirmed by us[11] have adopted a simple model Hamiltonian, considering a direct coupling between the Terbium spin and the Nickel magnetization. The present DFT results of the quenching of the spin radical upon direct contact with Ni substrate

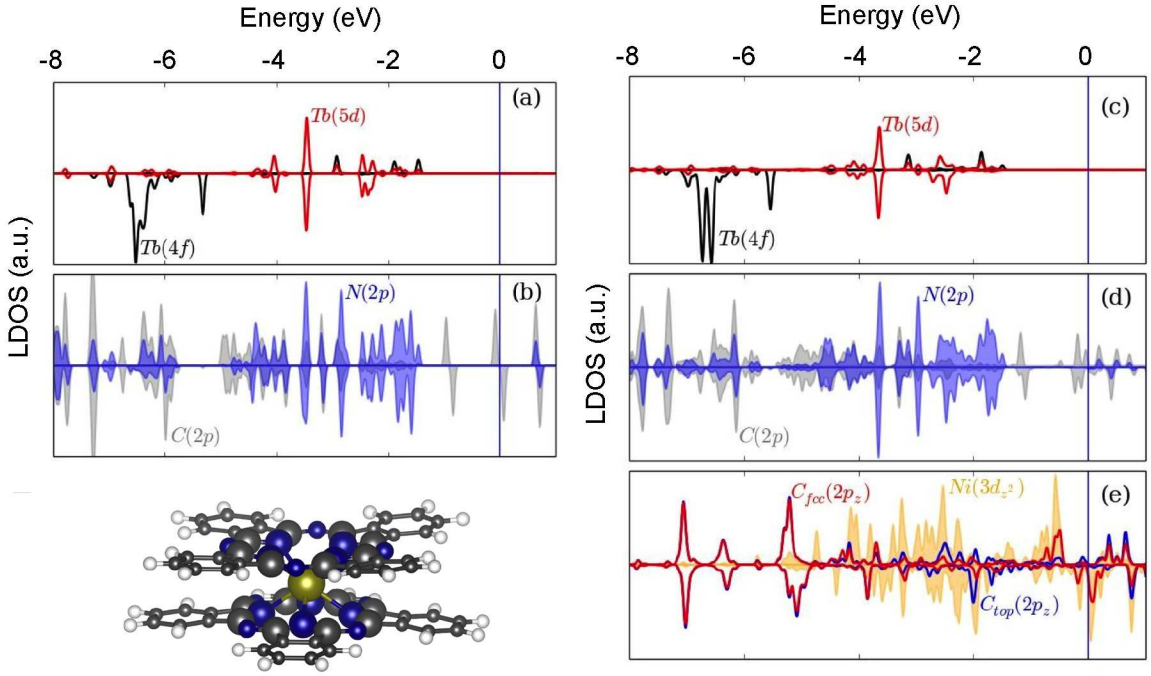

Figure 5: Spin-polarized LDOS of $TbPc_2$ in gas phase (a)−(b) and $TbPc_2$ on graphene/Ni(111) in the top-fcc stacking (c)−(e). (a)−(c) $4f$ and $5d$ states of Tb of $TbPc_2$; (b)−(d) the projections on the $2p$ orbitals of the nearest-neighbours to the Tb ion, N and C atoms (enlarged atoms in the molecule sketch); (e) $3d_{z^2}$ states of the first layer of Ni and $2p_z$ states of C_{top} and C_{fcc}. The d states of the Ni layer are plotted in orange, while graphene C p states are in blue and red. d−character in panels (a)−(c) has been enhanced for better comparison. In each panel, the upper (lower) side is relative to the majority (minority) spin channel (with respect to Ni), for the spin configuration depicted in Fig. 3.

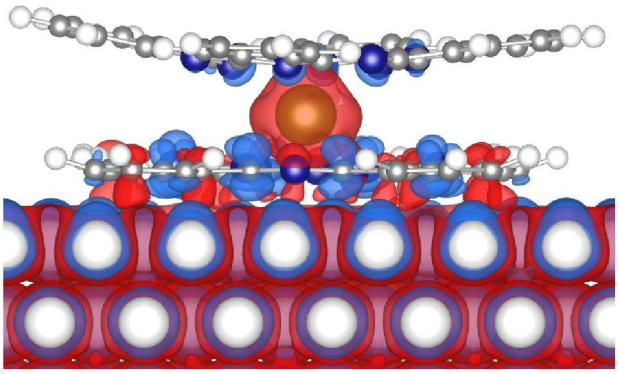

Figure 6: Side view of the spin-polarized charge density isosurfaces of $TbPc_2$ molecule adsorbed on Ni(111); blue (red) color stands for spin up (down) spin-polarization, relative to the positive (up) Ni magnetization (AFM coupling between Tb and Ni has been considered in the plot).

are in favor of this assumption. Thus, following the indications given by our DFT analysis, we propose for the $Tbpc_2$/graphene/Ni(111) system a spin model Hamiltonian where the spin radical is explicitly considered and has an active role in mediating the Tb-Ni coupling. The radical is portrayed as a spin-1/2, on the Pc_2 ligands, isotropically coupled to the spin of Terbium, to the magnetization of the Ni as well as to the external magnetic field. All the interactions described above are of electronic origin (*e.g.* superexchange), as we assume that dipolar interactions are much smaller, and in comparison, negligible.[16]

The model Hamiltonian describing the low-energy physics of the $TbPc_2$-graphene-Ni(111) system in an applied field $\mathbf{B}$ reads:

$$H_{\rm up} = H_{\rm CF} + \mu_B(\hat{\mathbf{L}} + 2\hat{\mathbf{S}} + 2\hat{\mathbf{s}}) \cdot \mathbf{B} + J_{\rm exch}\hat{\mathbf{S}} \cdot \hat{\mathbf{s}} + K\mathbf{M}_{\rm Ni} \cdot \hat{\mathbf{s}}, \quad (1)$$

In the above equation, $H_{\rm CF}$ is the crystal field Hamiltonian, $\hat{\mathbf{L}}$ and $\hat{\mathbf{S}}$ are the orbital and spin total angular momenta of the 4f-electrons in Tb^{3+}, $\hat{\mathbf{s}}$ the spin of the Pc radical, and $\mathbf{M}_{\rm Ni}$ the Ni magnetization. (The model Hamiltonian 1 is solved in the case of a Ni single crystal multidomain magnetic structure, as discussed in the Supporting Information). $J_{\rm exch}$ and K are parameters describing the magnetic exchange couplings between the Tb and Pc radical, and the Pc radical and the Ni magnetization, respectively.

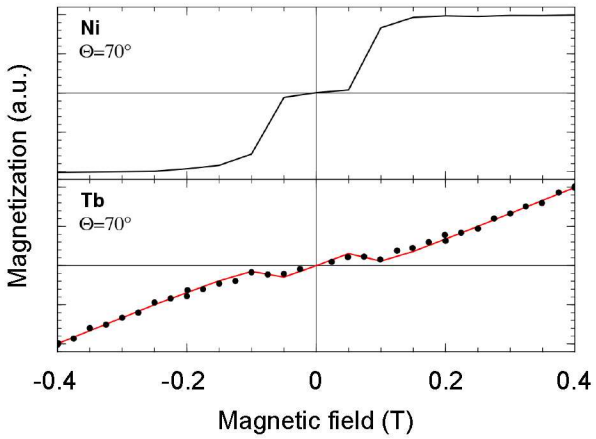

Figure 7: Zoom in on the low-field region of the XMCD magnetization of $TbPc_2$ on graphene/Ni(111) substrate, for $\Theta = 70°$ (dots). In the upper (lower) panels the Ni (Tb) magnetizations are displayed. The colored (red) line is the simulated Tb magnetization using Hamiltonian (1), with $J_{\rm exch} = -2.0$ cm^{-1}and $K = +1.8$ cm^{-1}.

In order to reduce the number of parameters in the model, we have evaluated the intramolecular interaction $J_{\rm exch}$ by CASSCF calculations, followed by spin–orbit (SO) diagonalization to account for the important effect of SO coupling on the Tb^{3+} centre (more details are given in the Method section). The calculations predict a ferromagnetic intramolecular Tb-radical exchange constant $J_{\rm exch} = -2.0\,{\rm cm}^{-1}$. If we assume the above value for $J_{\rm exch}$, it is possible to fit the experimental magnetization curve, as shown in Fig. 7, choosing a value of the radical-Ni coupling K of the same order of magnitude of $J_{\rm exch}$, but reversed in sign, *i.e.* $K = +1.8\,{\rm cm}^{-1}$. We note that, with the same choice of parameters, the model is able to fit also the Tb magnetization curve obtained at normal incidence, *i.e.* $\Theta = 0°$ (see blue dots and line in Fig. 2). In this case, the absence of a visible kink in the experimental and theoretical Tb magnetization is a direct consequence of the different magnetic behavior of the Ni substrate, for which the

magnetization saturates only for fields greater than 0.5 T (see the Supporting Information), as compared to the $\Theta = 70°$ case, where the onset of Ni saturation is at fields around ~ 0.2 T (see the upper panel in Fig. 7). Being the size of the magnetic coupling proportional to the Ni magnetization (see Eq. 1), and considering the reduced coupling induced by the presence of graphene, the signature of the magnetic coupling in the magnetization curves almost disappears for $\Theta = 0°$. The spin model described in the Hamiltonian of Eq. 1 encodes thus a relay-like Tb-spin radical-Ni exchange mechanism, which is able to reproduce, with realistic values of the coupling parameters, the magnetization cycles extracted by XMCD experiments.

Discussion

We discuss here in more detail the possible theoretical and experimental estimates of the exchange parameters K and $J_{\rm exch}$ in the Hamiltonian 1. If both the parameters are freely varied, the Tb magnetization curve could be fitted for a broad range of $[K, J]$ values, the system being somehow under-determined. This happens also in virtue of the very small coupling evidenced by the XMCD experiments which lead to a smooth behavior of the Tb magnetization signal, with only a small kink emerging wearily from the almost linear behavior shown at low applied field. An alternative approach, to the one discussed in the previous section, is to supply an estimate for K and find the $J_{\rm exch}$ which best fits the experiments. We have thus characterized by DFT, states with different spin alignments, with the radical coupled either ferro- or antiferromagnetically with the Ni substrate, and calculated the difference in the total energies of these states. We find that the residual spin polarization in the Pc planes couples ferromagnetically to the Ni magnetization, *i.e.* $K = -365\,{\rm cm}^{-1}$. We note that the magnitude of this coupling is rather significant considering that only $\pi - \pi$ interactions are present between the Pc and graphene planes, *i.e.* no direct chemical bonds form at the Pc-graphene interface, and that the distance between Pc and Ni is around 5.1 Å. If we assume for K the DFT value, *i.e.* $K = -365\,{\rm cm}^{-1}$, the model is still able to fit the experimental data, and the best fit is found for $J_{\rm exch} = +0.26\,{\rm cm}^{-1}$. Clearly, since the experimental findings prove an overall *indirect* antiferromagnetic coupling between Ni and Tb, the Tb-radical and radical-Ni couplings cannot be simultaneously ferromagnetic, so that the above first principle estimates of K and $J_{\rm exch}$, done by DFT and CASSCF respectively, could not be valid at the same time. From the theoretical point of view, a more precise and trustful numerical evaluation of the above couplings would require the employment of more advanced approaches, and their application to systems both complex and large as the ones considered in this work is not feasible at the current stage. Whereas there is no direct experimental evaluation of the radical-Ni coupling to compare with, the intramolecular Tb-radical coupling has been estimated, in indirect ways, by transport experiments in molecular spin-transistor[28,29] and spin-valve[3] geometries, or by combination of NMR experiments and DFT calculations.[30] The order of magnitude extracted from the experiments is in good agreement with the one coming from our fits. However, in the above experiments both ferro-[3,28,30] and antiferro-magnetic[29] coupling has been extracted, suggesting that the sign of the Tb-radical intramolecular coupling can be influenced by the experimental geometry and by the distortions that the molecules suffer when interacting with the substrate leads.

Conclusions

To summarize, we have presented a combined theoretical and experimental study of the magnetic interactions in $TbPc_2$ molecules adsorbed on graphene-decorated Ni substrates. Detailed DFT calculations, performed both in absence and presence of the graphene layer, give a rather strong indication that in the latter case, the spin radical on the Pc ring survives the interaction, the driving mechanism being the active role of graphene in electronically decoupling the molecule from the reactive Ni surface. We have

found instead a complete quenching of the radical when the molecule is directly in contact with the Ni. Following these indications, in the case of the $TbPc_2$/graphene/Ni(111) system, we propose a spin model Hamiltonian where the radical spin on the organic Pc ligands has an active role in mediating the antiferromagnetic interaction between Tb magnetic moment and the Ni magnetization. Such model accounts for the magnetization cycles measured in XMCD experiments. We have presented also theoretical estimates by DFT and CASSCF calculations of the different exchange interactions at play in the system, although the relative signs of the Tb-radical and radical-Ni couplings could not be univocally determined in the presented work.

Methods

XMCD experiments

$TbPc_2$ molecule evaporation is performed after degassing of the powders, keeping the evaporator temperature at 420°C and monitoring the thickness with an *in situ* quartz microbalance. XMCD measurements at the at the $L_{2,3}$ absorption edges of Ni and $M_{4,5}$ absorption edges of Tb were performed in total electron yield mode at a base pressure of 1.0 x 10^{-10} mbar The dichroic spectrum is the difference between the XAS spectra taken with the helicity of the incident photon antiparallel (I-) and parallel (I+) to the external field, normalized by the height of the XAS edge. Since the XAS and XMCD lineshapes do not change with the field, to record the magnetization curve we measured only the intensities of the $L_3(M_5)$ edge (E) at 853(1243) eV and pre-edge (P) at 845(1232) eV for the two polarizations; the resulting magnetization value is defined as: (E-/P- − E+/P+) / $\frac{1}{2}$ (E-/P- + E+/P+). For the magnetization measurements at $\Theta = 70°$ at the Tb M_5 edge, in order to highlight the tiny magnetic coupling, each point is obtained as the average between the curve recorded sweeping the field up and the curve recorded sweeping the field down, also averaging the absolute values of the points recorded with negative and positive fields.

Density-functional calculations

The DFT calculations have been performed by means of the Quantum Espresso (QE) computational package,[22] with the Perdew-Burke-Ernzerhof (PBE)[31] exchange correlation functional. We used the projector augmented wave method (PAW)[32] as recently implemented in the pseudopotentials made by Andrea Dal Corso,[33] with kinetic and charge density cutoffs of 1650 eV and 8440 eV, respectively. Simulating rare earths within DFT is very tricky, due to the strong electronic correlation effects in $4f$-electrons. In order to overcome this deficiency, DFT+U[34,35] or hybrid functionals[36–39] approaches are commonly employed. Since in our supercell calculation the molecule and the metal substrate must be treated on the same footing, for computational reasons, we have chosen the DFT+U method, using a value of U = 6 eV (obtained using the linear response approach of Cococcioni *et al.*[40]). No spin-orbit coupling is included in the calculations. Dispersion interactions have been included according to the DFT−D2 approach.[41] The convergence towards states with different spin distributions is achieved employing removable local and global magnetization constraints during electronic self-consistency cycles, as implemented in QE. The Ni slab is composed of five Ni monolayers, in the absence of graphene, while three Ni monolayers have been employed for the Gr/Ni(111) substrate. Relaxation of the atomic coordinates at the molecule/substrate interface has been considered (molecule + upper surface layer), till remnant forces on the atoms were of the order of 5 meV/Å.

CASSCF calculations

The *ab-initio* calculations were done on $[TbPc_2]^0$ in vacuum, using the DFT-optimized structure for that molecule adsorped on the graphene/Ni surface. We used ANO-RCC basis sets from the Molcas library, contracted to VDZP on Tb and VDZ on C, N, and H. The active space in the CASSCF calculation con-

sists of nine electrons in eight orbitals: eight electrons and seven 4f orbitals from Tb^{3+} plus one electron and the highest occupied π-orbital from Pc_2. In a SO-free picture, the spin-1/2 of the Pc electron couples with the spin-3 of the ^7F Hund ground state of Tb^{3+} into two total-spin states, $S = 5/2$ and $S = 7/2$. For each of these we performed a state-averaged CASSCF calculation over the seven lowest states, formally corresponding to the sevenfold orbital degeneracy of ^7F, but now split by the crystal field of the ligand. We obtain the exchange splitting by taking the difference between the total ground-state energies of $S = 7/2$ and $S = 5/2$. This resulted in a calculated ferromagnetic stabilization of $S = 7/2$ over $S = 5/2$ by 7 cm^{-1}. Next we introduce SO coupling in the basis of the CASSCF wavefunctions using an atomic mean-field approximation of the SO operator, which is implemented in Molcas's RASSI module. This results in states that can be identified as coming from the $J = 6$ ground multiplet of Tb^{3+}, split by the crystal field, and weakly coupled to the radical spin. Analysis of the calculated wavefunctions reveals that the radical is coupled ferromagnetically to the Ising doublet $|M_J = \pm 6\rangle$, with an exchange gap of 6 cm^{-1}. The first excited crystal field state is calculated at 313 cm^{-1}, well above the ground state.

Acknowledgement This work has been partially supported by European Community through the FET-Proactive Project MoQuaS, contract N.610449 and by the Italian Ministry for Research (MIUR) through the FIR grant RBFR13YKWX, and PRIN grant 20105ZZTSE "GRAF". A. Soncini and M. Affronte acknowledge financial support from the Australian Research Council Discovery Project Grant DP150103254. We also acknowledge the European Synchrotron Radiation Facility (Project HE 3739) and we would like to thank the beamline staff for assistance in using beamline ID08. Computation time at CINECA supercomputing centers is also gratefully acknowledged.

Supporting Information Available: DFT calculation of $TbPc_2$ on top-bridge stacked graphene/Ni(111) substrates; Implementation the spin-model Hamiltonian for the multi-domain magnetic structure of Ni single crystal; approximated spin-model Hamiltonian following CASSCF calculations; XPS and XLND characterization of the $TbPc_2$ film; XAS and XMCD spectra and magnetization cycle of Ni single crystal. This material is available free of charge via the Internet at `http://pubs.acs.org/`.

References

1. Bogani, L.; Wernsdorfer, W. Molecular Spintronics using Single-Molecule Magnets. *Nat. Mater.* **2008**, *7*, 179–186.

2. Urdampilleta, M.; Klyatskaya, S.; Cleuziou, J.-P.; Ruben, M.; Wernsdorfer, W. Supramolecular Spin Valves. *Nat. Mater.* **2011**, *10*, 502–506.

3. Urdampilleta, M.; Klayatskaya, S.; Ruben, M.; Wernsdorfer, W. Magnetic Interaction between a Radical Spin and a Single-Molecule Magnet in a Molecular Spin-Valve. *ACS Nano* **2015**, *9*, 4458–4464.

4. Ishikawa, N.; Sugita, M.; Wernsdorfer, W. Quantum Tunneling of Magnetization in Lanthanide Single-Molecule Magnets: Bis(phthalocyaninato)terbium and Bis(phthalocyaninato)dysprosium Anions. *Angew. Chem., Int. Ed.* **2005**, *44*, 2931–2935.

5. Ishikawa, N. Single Molecule Magnet with Single Lanthanide Ion. *Polyhedron* **2007**, *26*, 2147–2153.

6. Rizzini, A. L.; Krull, C.; Mugarza, A.; Balashov, T.; Nistor, C.; Piquerel, R.; Klyatskaya, S.; Ruben, M.; Sheverdyaeva, P. M.; Moras, P.; Carbone, C.; Stamm, C.; Miedema, P. S.; Thakur, P. K.; Sessi, V.; Soares, M.; Yakhou-Harris, F.; Cezar, J. C.; Stepanow, S.; Gambardella, P. Coupling of Single, Double, and Triple-Decker

Metal-Phthalocyanine Complexes to Ferromagnetic and Antiferromagnetic Substrates. *Surf. Sci.* **2014**, *630*, 361–374.

7. Annese, E.; Fujii, J.; Vobornik, I.; Panaccione, G.; Rossi, G. Control of the Magnetism of Cobalt Phthalocyanine by a Ferromagnetic Substrate. *Phys. Rev. B* **2011**, *84*, 174443.

8. Klar, D.; Klyatskaya, S.; Candini, A.; Krumme, B.; Kummer, K.; Ohresser, P.; Corradini, V.; de Renzi, V.; Biagi, R.; Joly, L.; Kappler, J.-P.; del Pennino, U.; Affronte, M.; Wende, H.; Ruben, M. Antiferromagnetic Coupling of $TbPc_2$ Molecules to Ultrathin Ni and Co Films. *Beilstein J. Nanotechnol.* **2013**, *4*, 320–324.

9. Candini, A.; Bellini, V.; Klar, D.; Corradini, V.; Biagi, R.; De Renzi, V.; Kummer, K.; Brookes, N. B.; del Pennino, U.; Wende, H.; Affronte, M. Ferromagnetic Exchange Coupling between Fe Phthalocyanine and Ni(111) Surface Mediated by the Extended States of Graphene. *J. Phys. Chem. C* **2014**, *118*, 17670–17676.

10. Rajaraman, G.; Totti, F.; Bencini, A.; Caneschi, A.; Sessoli, R.; Gatteschi, D. Density Functional Studies on the Exchange Interaction of a Dinuclear Gd(III)-Cu(II) Complex: Method Assessment, Magnetic Coupling Mechanism and Magneto-Structural Correlations. *Dalton Trans.* **2009**, 3153–3161.

11. Candini, A.; Klar, D.; Marocchi, S.; Corradini, V.; Biagi, R.; de Renzi, V.; del Pennino, U.; Troiani, F.; Bellini, V.; Klyatskaya, S.; Ruben, M.; Kummer, K.; Brookes, N. B.; Huang, H.; Soncini, A.; Wende, H.; Affronte, M. Spin-Communication Channels between Ln(III) Bis-Phthalocyanines Molecular Nanomagnets and a Magnetic Substrate. *Sci. Rep.* **2016**, *6*, 21740.

12. Branzoli, F.; Carretta, P.; Filibian, M.; Klyatskaya, S.; Ruben, M. Low-Energy Spin Dynamics in the $[YPc_2]^0$ $S = \frac{1}{2}$ Antiferromagnetic Chain. *Phys. Rev. B* **2011**, *83*, 174419.

13. Vitali, L.; Fabris, S.; Conte, A. M.; Brink, S.; Ruben, M.; Baroni, S.; Kern, K. Electronic Structure of Surface-Supported Bis(Phthalocyaninato) Terbium(III) Single Molecular Magnets. *Nano Lett.* **2008**, *8*, 3364–3368.

14. Komeda, T.; Isshiki, H.; Liu, J.; Zhang, Y.-F.; Lorente, N.; Katoh, K.; Breedlove, B. K.; Yamashita, M. Observation and Electric Current Control of a Local Spin in a Single-Molecule Magnet. *Nat. Commun.* **2011**, *2*, 217.

15. Schwoebel, J.; Fu, Y.; Brede, J.; Dilullo, A.; Hoffmann, G.; Klyatskaya, S.; Ruben, M.; Wiesendanger, R. Real-Space Observation of Spin-Split Molecular Orbitals of Adsorbed Single-Molecule Magnets. *Nat. Commun.* **2012**, *3*, 953.

16. Lodi Rizzini, A.; Krull, C.; Balashov, T.; Kavich, J. J.; Mugarza, A.; Miedema, P. S.; Thakur, P. K.; Sessi, V.; Klyatskaya, S.; Ruben, M.; Stepanow, S.; Gambardella, P. Coupling Single Molecule Magnets to Ferromagnetic Substrates. *Phys. Rev. Lett.* **2011**, *107*, 177205.

17. Lodi Rizzini, A.; Krull, C.; Balashov, T.; Mugarza, A.; Nistor, C.; Yakhou, F.; Sessi, V.; Klyatskaya, S.; Ruben, M.; Stepanow, S.; Gambardella, P. Exchange Biasing Single Molecule Magnets: Coupling of $TbPc_2$ to Antiferromagnetic Layers. *Nano Lett.* **2012**, *12*, 5703–5707.

18. Stepanow, S.; Honolka, J.; Gambardella, P.; Vitali, L.; Abdurakhmanova, N.; Tseng, T.-C.; Rauschenbach, S.; Tait, S. L.; Sessi, V.; Klyatskaya, S.; Ruben, M.; Kern, K. Spin and Orbital Magnetic Moment Anisotropies of Monodispersed Bis(Phthalocyaninato)Terbium on a Copper Surface. *J. Am. Chem. Soc.* **2010**, *132*, 11900–11901.

19. Margheriti, L.; Chiappe, D.; Mannini, M.; Car, P.-E.; Sainctavit, P.; Arrio, M.-A.; de Mongeot, F. B.; Cezar, J. C.; Piras, F. M.; Magnani, A.; Otero, E.; Caneschi, A.; Sessoli, R. X-Ray Detected Magnetic Hysteresis of Thermally Evaporated Terbium Double-Decker Oriented Films. *Adv. Mater.* **2010**, *22*, 5488–5493.

20. Gonidec, M.; Biagi, R.; Corradini, V.; Moro, F.; De Renzi, V.; del Pennino, U.; Summa, D.; Muccioli, L.; Zannoni, C.; Amabilino, D. B.; Veciana, J. Surface Supramolecular Organization of a Terbium(III) Double-Decker Complex on Graphite and its Single Molecule Magnet Behavior. *J. Am. Chem. Soc.* **2011**, *133*, 6603–6612.

21. Klar, D.; Candini, A.; Joly, L.; Klyatskaya, S.; Krumme, B.; Ohresser, P.; Kappler, J.-P.; Ruben, M.; Wende, H. Hysteretic Behaviour in a Vacuum Deposited Submonolayer of Single Ion Magnets. *Dalton Trans.* **2014**, *43*, 10686–10689.

22. Giannozzi, P.; Baroni, S.; Bonini, N.; Calandra, M.; Car, R.; Cavazzoni, C.; Ceresoli, D.; Chiarotti, G. L.; Cococcioni, M.; Dabo, I.; Dal Corso, A.; de Gironcoli, S.; Fabris, S.; Fratesi, G.; Gebauer, R.; Gerstmann, U.; Gougoussis, C.; Kokalj, A.; Lazzeri, M.; Martin-Samos, L. *et al.* QUANTUM ESPRESSO: a Modular and Open-Source Software Project for Quantum Simulations of Materials. *J. Phys.: Condens. Matter* **2009**, *21*, 395502.

23. Zhao, W.; Kozlov, S. M.; Höfert, O.; Gotterbarm, K.; Lorenz, M. P. A.; Viñes, F.; Papp, C.; Görling, A.; Steinrück, H.-P. Graphene on Ni(111): Coexistence of Different Surface Structures. *J. Phys. Chem. Lett.* **2011**, *2*, 759–764.

24. Gamo, Y.; Nagashima, A.; Wakabayashi, M.; Terai, M. Atomic Structure of Monolayer Graphite Formed on Ni (111). *Surf. Sci.* **1997**, *374*, 61.

25. Bianchini, F.; Patera, L. L.; Peressi, M.; Africh, C.; Comelli, G. Atomic Scale Identification of Coexisting Graphene Structures on Ni(111). *J. Phys. Chem. Lett.* **2014**, *5*, 467–473.

26. Marocchi, S.; Ferriani, P.; Caffrey, N. M.; Manghi, F.; Heinze, S.; Bellini, V. Graphene-Mediated Exchange Coupling between a Molecular Spin and Magnetic Substrates. *Phys. Rev. B* **2013**, *88*, 144407.

27. Katoh, K.; Yoshida, Y.; Yamashita, M.; Miyasaka, H.; Breedlove, B. K.; Kajiwara, T.; Takaishi, S.; Ishikawa, N.; Isshiki, H.; Zhang, Y. F.; Komeda, T.; Yamagishi, M.; Takeya, J. Direct Observation of Lanthanide(III)-Phthalocyanine Molecules on Au(111) by Using Scanning Tunneling Microscopy and Scanning Tunneling Spectroscopy and Thin-Film Field-Effect Transistor Properties of Tb(III)- and Dy(III)-Phthalocyanine Molecules. *J. Am. Chem. Soc.* **2009**, *131*, 9967–9976.

28. Vincent, R.; Klyatskaya, S.; Ruben, M.; Wernsdorfer, W.; Balestro, F. Electronic Read-Out of a Single Nuclear Spin Using a Molecular Spin Transistor. *Nature* **2012**, *488*, 357–360.

29. Thiele, S.; Balestro, F.; Ballou, R.; Klyatskaya, S.; Ruben, M.; Wernsdorfer, W. Electrically Driven Nuclear Spin Resonance in Single-Molecule Magnets. *Science* **2014**, *344*, 1135–1138.

30. Damjanović, M.; Morita, T.; Katoh, K.; Yamashita, M.; Enders, M. Ligand π Radical Interaction with F-Shell Unpaired Electrons in Phthalocyaninato-Lanthanoid Single-Molecule Magnets: a Solution NMR Spectroscopic and DFT Study. *Chem. - Eur. J.* **2015**, *21*, 14421–14432.

31. Perdew, J. P.; Burke, K.; Ernzerhof, M. Generalized Gradient Approximation Made Simple. *Phys. Rev. Lett.* **1996**, *77*, 3865.

32. Blöchl, P. E. Projector Augmented-Wave Method. *Phys. Rev. B* **1994**, *50*, 17953.

33. Corso, A. D. Pseudopotentials Periodic Table: From H to Pu. *Computational Materials Science* **2014**, *95*, 337 – 350.

34. Anisimov, V. I.; Zaanen, J.; Andersen, O. K. Band Theory and Mott Insulators: Hubbard U Instead of Stoner I. *Phys. Rev. B* **1991**, *44*, 943–954.

35. Liechtenstein, A. I.; Anisimov, V. I.; Zaanen, J. Density-Functional Theory and Strong Interactions: Orbital Ordering in Mott-Hubbard Insulators. *Phys. Rev. B* **1995**, *52*, R5467–R5470.

36. Becke, A. D. A New Mixing of Hartree-Fock and Local Density-Functional Theories. *J. Chem. Phys.* **1993**, *98*, 1372–1377.

37. Perdew, J. P.; M., E.; Burke, K. Rationale for Mixing Exact Exchange with Density Functional Approximations. *J. Chem. Phys.* **1996**, *105*, 9982–9985.

38. Cinquini, F.; Giordano, L.; Pacchioni, G.; Ferrari, A. M.; Pisani, C.; Roetti, C. Electronic Structure of NiO/Ag(100) Thin Films from DFT+U and Hybrid Functional DFT Approaches. *Phys. Rev. B* **2006**, *74*, 165403.

39. Adamo, C.; Barone, V.; Bencini, A.; Totti, F.; Ciofini, I. On the Calculation and Modeling of Magnetic Exchange Interactions in Weakly Bonded Systems: The Case of the Ferromagnetic Copper(II) μ2-Azido Bridged Complexes. *Inorg. Chem.* **1999**, *38*, 1996–2004.

40. Cococcioni, M.; de Gironcoli, S. Linear Response Approach to the Calculation of the Effective Interaction Parameters in the LDA + U Method. *Phys. Rev. B* **2005**, *71*, 035105.

41. Grimme, S.; Antony, J.; Ehrlich, S.; Krieg, H. A Consistent and Accurate *Ab-Initio* Parametrization of Density Functional Dispersion Correction (DFT-D) for the 94 Elements H-Pu. *J. Chem. Phys.* **2010**, *132*, 154104.

Graphical TOC Entry